

# EMOS Platform: Real-Time Capacity Estimation of MIMO Channels in the UMTS-TDD Band

Raul de Lacerda <sup>#1</sup>, Leonardo Sampaio Cardoso <sup>#2</sup>, Raymond Knopp <sup>#3</sup>, David Gesbert <sup>#4</sup>, Mérouane Debbah <sup>\*5</sup>

<sup>#</sup>Communication Department, Eurecom Institute  
2229, Rt des Crêtes - B.P. 193, 06904 Sophia Antipolis, France

<sup>1</sup>raul.de-lacerda@eurecom.fr

<sup>2</sup>leonardo.sampaio@eurecom.fr

<sup>3</sup>raymond.knopp@eurecom.fr

<sup>4</sup>david.gesbert@eurecom.fr

<sup>\*</sup>Supelec

91190, Gif-sur-Yvette, France

<sup>5</sup>merouane.debbah@supelec.fr

**Abstract**—This work presents some initial results concerning the MIMO channel capacity of real wireless channels in the UMTS-TDD band using the Eurecom MIMO Openair Sounder (EMOS). This paper describes the necessary steps to estimate in real-time the wireless MIMO environment, offering the possibility to identify reliable MIMO channels as well as instantaneous channel capacity. In particular, the problems related to additive and phase-shift noise are solved by employing OFDMA technology. Finally, based on measurements, we analyze the impact of polarization on the capacity performance.

## I. INTRODUCTION

During the last years, many studies were developed to investigate the capacity offered by Multiple-Input Multiple-Output (MIMO) systems [1], [2], [3]. By exploiting the multipath propagation channel, multiple antenna systems were shown to significantly increase the performance of single antenna systems, also known as Single-Input Single-Output (SISO) systems. As a consequence, single user MIMO systems have gained more and more attention.

In order to analyze the MIMO gains, Eurecom Institute has developed a MIMO platform called Eurecom MIMO Openair Sounder (EMOS) which employs 4 transmit antennas and 2 receive antennas. The main idea behind EMOS is to carry out real MIMO channel measurements on a real-time basis, unlike [4]. EMOS is capable of providing real time measurements with polarization and adjustable antenna spacing. This work presents some initial results concerning the MIMO channel capacity of real wireless channels in the UMTS-TDD band using Eurecom MIMO Openair Sounder (EMOS). This paper describes the necessary steps to estimate in real-time the wireless MIMO environment, offering the possibility to identify reliable MIMO channels as well as the instantaneous channel capacity. Finally, based on the measurements, we analyze the impact of polarization on the capacity performance.

In section II, we present the EMOS platform, showing all of its main characteristics and parameters. Next, in section III,

we present the procedures developed to estimate the channel. In section IV, initial measurements results using the EMOS are presented. Finally, some conclusions and perspectives are drawn in section V.

Throughout this paper, we use lower case letters to represent scalars and bold lower case letters to represent vectors. The superscripts  $\dagger$  denote the hermitian of the matrix argument.  $I_n$  is the identity matrix of size  $n \times n$ .  $E\{\cdot\}$  is the expectation operator.  $\mathbf{X} = (x_{ij})_{i=1, \dots, n_1}^{j=1, \dots, n_2}$  is the  $n_1 \times n_2$  matrix whose  $(i, j)$ -element is the scalar  $x_{ij}$ .

## II. EURECOM MIMO OPENAIR SOUNDER (EMOS)

EMOS is a real-time platform able to carry out real transmissions using the UMTS-TDD band. Based on the OpenAir system developed at Eurecom [5], [6], EMOS is able to operate in real-time dealing with real RF signals. It is developed with the purpose to create an ideal architecture for experimenting with real wireless environments as well as analytical results validation.



(a) Base Station server.

(b) Powerwave Antenna.

Fig. 1. Base-station antenna configuration.

The platform consists of a base-station that sends a signaling frame continuously, and some (one or more) terminals that

TABLE I  
POWERWAVE ANTENNA (PART NO. 7760.00)

Parameter	Value
Frequency range (MHz)	1710-2170
Frequency band (MHz)	(1710-1800) (1850-1900) (1900-2025) (2110-2170)
Electrical downtilt	0° to 8°
Number of elements	4

TABLE II  
PANORAMA ANTENNA (PART NO. TCLIP-DE3G)

Parameter	Value
Frequency range (MHz)	(824-960) (1710-2170)
Frequency band	(GSM850) (GSM900) (GSM1800) (GSM1900) (3G UMTS)

receive the frames to estimate the channel. For the base-station (see Fig. 1(a)), an ordinary server PC is employed with four PLATON Cards<sup>1</sup> [7], where each card is connected to a power amplifier which feeds an antenna. As far as the terminals are concerned, an ordinary laptop computer is used along with Eurecom's dual-RF CardBus/PCMCIA card [8], which allow to employ two antennas for two-way real-time experimentation.

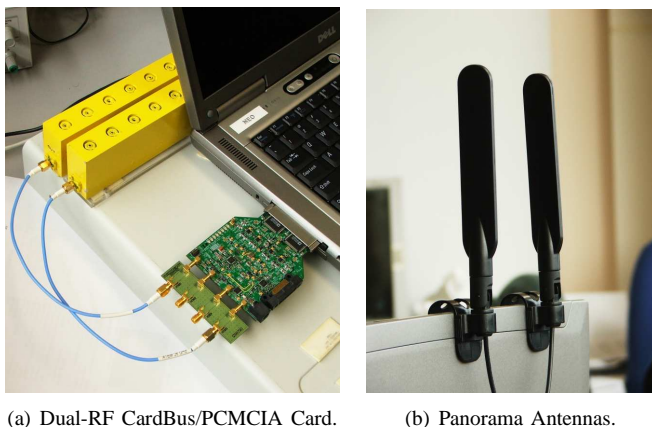


Fig. 2. Terminal antenna configuration.

### A. Antenna Settings

The antenna employed at the base-station is the Powerwave part no. 7760.00 (see Fig. 1(b)). It is a 3G broadband antenna composed of four elements which are arranged in two cross-polarized pairs. The main parameters concerning the base-station antenna are listed in Table I.

The antennas employed at the terminal are the Panorama Antennas, part no. TCLIP-DE3G (see Fig. 2(b)). It is basically a 3G antenna with a clip mount for laptop computers. The main parameters concerning the terminal antenna are listed in Table II.

<sup>1</sup>The PLATON cards were originally built as an UMTS-TDD testbed and include much more functionalities than required for EMOS.

### B. Transmit Frame

Although originally based on the UMTS-TDD standard, recent developments have pushed the Eurecom's team to use an OFDMA based signaling. Hence, at the base-station, four data sequences are transmitted in parallel, i.e., each TX chain has its own sequence. To simplify the processing complexity at the receiver, four frequency-orthogonal sequences were employed.

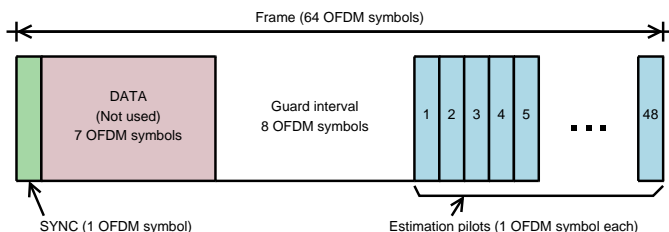


Fig. 3. Frame Structure.

The transmit frame is illustrated in Fig. 3. Because of the constant variation of the wireless channel and in order to take into account the coherence time of the channel, we considered a small frame (the frame duration is approximately of 2.5ms). For a reliable estimation, we divided the frame in 64 packets, where each packet represents an OFDM symbol composed only by 320 symbols (256 useful symbols and 64 symbols of cyclic prefix, which give 64 symbols for each TX chain). For processing purposes, the frame is constituted by 4 different kinds of data:

- The first part of the frame is composed of one single OFDM symbol. This symbol has a special structure that permits the terminal to easily synchronize with the base-station.
- The second part of the frame is composed of useful data. For the moment, it is not used.
- The third part is composed of zeros. This part is used to estimate the noise characteristics.
- The fourth and last part of the frame, is composed of a sequence of OFDM pilot symbols.

### C. Receiver Processing

At the receiver, the terminal does the frame synchronization procedure and suppresses the phase-shift noise generated by the dual-RF CardBus/PCMCIA card. After that, it estimates the MIMO channel for channel capacity analysis.

1) *Frame Synchronization*: The first step of the receiver processing is the frame synchronization. At this step, the receiver stores the received data in a memory with twice the size of a frame. After that, the receiver does a correlation analysis between the received data and the OFDM symbol dedicated to the synchronization purpose. Then, the synchronization is decided based on the position of the maximum value resulting from that correlation.

It is important to notice that for the moment, this synchronization procedure is employed for each frame, with the

objective to guarantee that no error due to synchronization will occur during the channel estimation and/or capacity analysis.

2) *Phase-Shift Noise Suppression*: The second step of the receiver processing is the phase-shift noise suppression. Generated by the RF circuit, the phase-shift noise was observed to have a slow variation characteristic. For this reason, to guarantee a good phase-shift suppression for the received signal at each receive antenna, we mitigate the phase shift for each OFDM pilot symbol of each frame.

Assuming that  $\mathbf{y}^{(k)}$  is the received OFDM pilot symbol vector ( $1 \times 320$ ) of the  $k$ th OFDM pilot symbol of the received frame, where  $17 \leq k \leq 64$ . We model the phase-shift noise as being constant for each OFDM symbol and different for different OFDM symbols, which turns out to be a good model for the Eurecom's dual-RF CardBus/PCMCIA. For the noise-shift suppression, first the ratio between the phase-shift of the first OFDM pilot symbol ( $k = 17$ ) and all the other pilots are estimated by the following equation:

$$v^{(k)} = \frac{1}{320} \sum_{a=1}^{320} \frac{\mathbf{y}^{(17)}[a]}{\mathbf{y}^{(k)}[a]}. \quad (1)$$

After that, we multiply each vector  $\mathbf{y}^{(k)}$  by the respective normalized and estimated phase-offset  $v^{(k)}$ , which give us a constant phase-shift for each frame

$$\mathbf{y}_{new}^{(k)} = v^{(k)} \cdot \mathbf{y}_{old}^{(k)}. \quad (2)$$

3) *Channel Estimation*: The next step is the most important one and it concerns the estimation of the MIMO channel. To diminish the effects of the white noise, each OFDM pilot is used to estimate the MIMO channel and all estimations of one frame are averaged. As a consequence, a reliable MIMO channel estimation is obtained per frame.

Consider  $\mathbf{x}$  as being the transmitted signal,  $\mathbf{H}$  the MIMO channel matrix,  $\mathbf{n}$  the additive white gaussian noise and  $\mathbf{y}$  the received signal, the system model can be represented in frequency by the following equation

$$\mathbf{y}_i^{(k)}[f] = \mathbf{H}_i^{(k)}[f] \mathbf{x}^{(k)}[f] + \mathbf{n}_i^{(k)}[f] \quad (3)$$

where  $i$  represents the frame index,  $k$  represents the index of an OFDM symbol of a frame,  $f$  represents the discrete and normalized frequency generated by the OFDM signaling,  $\mathbf{y}_i^{(k)}[f]$ ,  $\mathbf{x}^{(k)}[f]$  and  $\mathbf{n}_i^{(k)}[f]$  are respectively the received vector ( $N_r \times 1$ ), the transmitted symbol vector ( $N_t \times 1$ ) and the AWGN vector ( $N_t \times 1$ ), and  $\mathbf{H}_i^{(k)}[f]$  is the channel matrix ( $N_r \times N_t$ ).

By using the OFDM signaling properties, the MIMO channel matrix estimated by each transmitted OFDM pilot is given by

$$\bar{\mathbf{H}}_i^{(k)}[f]_{(rx,tx)} = \frac{\mathbf{y}_i^{(k)}[f]_{(tx)}}{\mathbf{x}_{PILOT}^{(k)}[f]_{(tx)}} \quad (4)$$

$$= \frac{\mathbf{H}_i^{(k)}[f]_{(rx,tx)} \mathbf{x}^{(k)}[f]_{(tx)} + \mathbf{n}_i^{(k)}[f]_{(rx)}}{\mathbf{x}_{PILOT}^{(k)}[f]_{(tx)}} \quad (5)$$

$$= \mathbf{H}_i^{(k)}[f]_{(rx,tx)} + \frac{\mathbf{n}_i^{(k)}[f]_{(rx)}}{\mathbf{x}_{PILOT}^{(k)}[f]_{(tx)}} \quad (6)$$

where  $rx$  and  $tx$  represents respectively the receive and the transmit antennas.

To mitigate the noise of the channel estimation procedure, we average all the 48 channel estimations of one frame. Assuming that the channel is constant during the transmission of one frame (the expected coherence time of our measurements is around 10ms), we have that

$$\mathbb{E}[\bar{\mathbf{H}}_i^{(k)}[f]_{(rx,tx)}] = \mathbb{E} \left[ \mathbf{H}_i^{(k)}[f]_{rx,tx} + \frac{\mathbf{n}_i^{(k)}[f]_{rx}}{\mathbf{x}_{PILOT}^{(k)}[f]_{tx}} \right] \quad (7)$$

$$\bar{\mathbf{H}}_i[f]_{(rx,tx)} = \mathbb{E} \left[ \mathbf{H}_i^{(k)}[f]_{(rx,tx)} \right] + \mathbb{E} \left[ \frac{\mathbf{n}_i^{(k)}[f]_{(rx)}}{\mathbf{x}_{PILOT}^{(k)}[f]_{(tx)}} \right] \quad (8)$$

$$= \mathbf{H}_i^{(k)}[f]_{(rx,tx)} + \frac{1}{48} \sum_{i=1}^{48} \frac{\mathbf{n}_i^{(k)}[f]_{(rx)}}{\mathbf{x}_{PILOT}^{(k)}[f]_{(tx)}} \quad (9)$$

and for high SNR, we have

$$\bar{\mathbf{H}}_i[f] \cong \mathbf{H}_i^{(k)}[f] \quad (10)$$

4) *MIMO Capacity Analysis*: The last step of the receiver processing is the MIMO capacity estimation. Based on the classical results available in the literature [1], [2], we calculate the capacity by analyzing the estimated MIMO channel matrix. The result gives us an estimated capacity per frequency

$$C_i[f] = \log_2 \left[ \det \left( \mathbf{I}_2 + \frac{\rho}{4} \bar{\mathbf{H}}_i[f] \bar{\mathbf{H}}_i^\dagger[f] \right) \right] \quad (11)$$

where  $\rho$  is the signal-to-noise ratio (SNR) for each receiver chain. As one can see, for the capacity analysis, the constant phase-shift of each frame ( $v^{(k)}$ ) does not affect the capacity because it disappears during the calculation of the capacity. For the analysis presented in this paper, two different capacity results are considered: 1) Assuming a given SNR, which means that the columns of the channel are normalized; 2) Assuming the real SNR, which means that after the channel normalization we analyze the capacity for the estimated SNR.

### III. MEASUREMENT

As described before, the analysis conducted in this paper are based on the transmission from the base-station with four transmit antennas to the terminal with two receive antennas. On the analysis, along with 4x2 MIMO architecture, we also show the capacity performance obtained when 2x2 and 1x1 antenna combination is considered. The main radio characteristics adopted by EMOS for this measurement are listed in the Table III

TABLE III  
MEASUREMENT CHARACTERISTICS

Parameter	Value
Center frequency	1907.6 MHz
Bandwidth	5 MHz
Base-Station Tx Power	34 dBm
Number of Tx Antennas	4
Number of Rx Antennas	2

### A. Environment

For the measurement, an outdoor scenario very close to Eurecom Institute is considered, which is characterized by a semi-urban hilly environment, composed by short buildings and vegetation (see Fig. 4). The base-station antenna is situated in one of the highest buildings of the region and has a direct view of the environment. The outdoor measurements were conducted in a parking very close to the buildings that we see in the figure.



Fig. 4. View from the Base-Station.

### B. Polarization

For the capacity evaluation, two different kinds of polarizations are considered. The goal is to analyze the impact of the use of co-polarized antennas with space diversity and cross-polarized co-located antennas at the transmitter. The considered transmit structures are shown in Fig. 5. For the case where we have 4 transmit antennas, it is considered the two pairs of co-polarized/cross-polarized antennas.

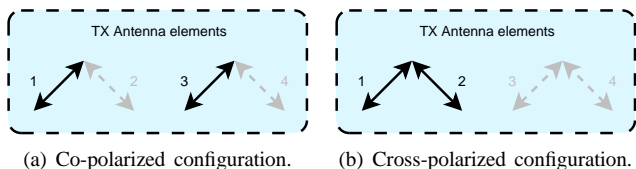


Fig. 5. Transmit antenna polarizations.

## IV. SOME RESULTS

In this section we present some measurements performed in an outdoor environment. The purpose of these results is to show the impact of the transmit architecture (number of antennas and/or polarization). Furthermore, we can evaluate the gains offered by the use of MIMO structures in a usual realistic environment. For this reason, we analyze the achievable capacity when we employ not only a  $4 \times 2$  MIMO, but also assuming other antenna combinations:  $1 \times 1$  MIMO,  $2 \times 2$  MIMO with co-polarized antennas at the transmitter,  $2 \times 2$  MIMO with cross-polarized antennas at the transmitter. The results presented here represent only an illustrative measurement campaign made with the EMOS platform and performed at the route shown in Fig. 6.



Fig. 6. Route where the measurements were performed.

At the receiver, the MIMO channel is estimated and the instantaneous capacity is derived as described before. In Fig. 7, an estimated channel between the transmit antenna 1 and the receiver antenna 1 is shown (for each pair of transmit-receive antennas an estimated matrix like the one presented in the figure is obtained). As it can be noted, a route with constant channel characteristics and with a good SNR ( $\approx 30dB$ ) was chosen. The measurement was performed at a storage rate of a frame at each 0.1s and with a receive antenna space equal to  $\lambda/2$ .

The plot shown in Fig. 8 shows the instantaneous capacity achieved by each frame over the measurement run. This result is obtained by the capacity average among all considered frequencies. As it can be noted, the average behavior of the capacity for all antenna combinations follows the signal fluctuation due to the path loss and fast fading.

The capacity CDF shown in Fig. 9 assumes a constant receive SNR of 10dB and an average of the obtained capacity among different frequencies. Furthermore, we also plotted the achievable capacities when i.i.d. MIMO channels randomly generated are considered.

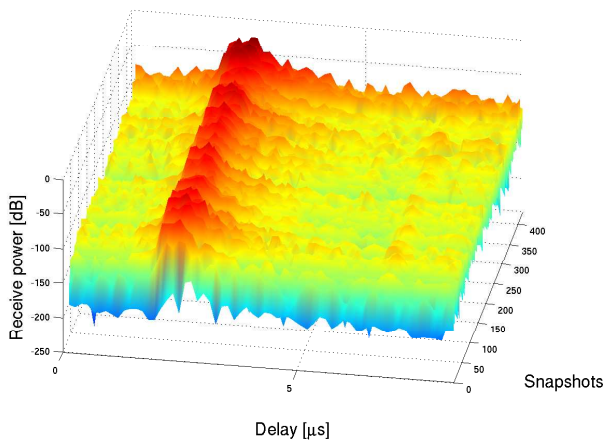


Fig. 7. Estimated channel over measurement (TX1 - RX1).

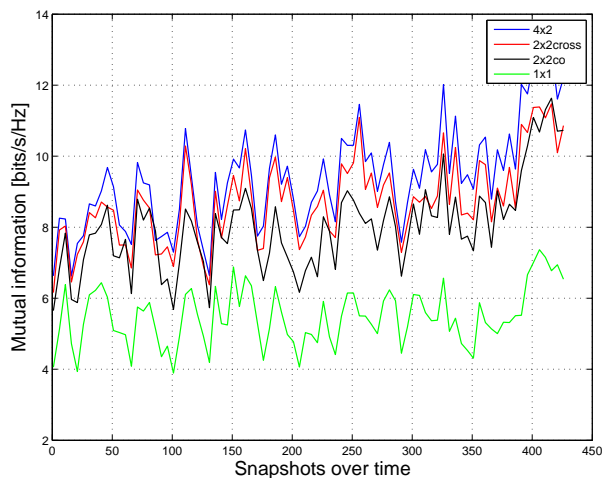


Fig. 8. Capacity over measurement (actual frame SNR).

As it can be seen, the real environment performs worse than the i.i.d. MIMO channels. It can also be seen that the use of MIMO increases the capacity when we compare it with the SISO case. It is important to note that the gain offered by the use of  $2 \times 2$  MIMO is really important, almost doubling the SISO capacity. In the other hand, increasing the number of antennas in this environment for more than 2 antennas at the transmitter does not yield in a further increase. Another important conclusion of the presented result is that we see an important gain when a cross-polarization antenna is used as compared with the obtained capacity when co-polarized antennas are used at the transmitter.

## V. CONCLUSIONS AND PERSPECTIVES

In this paper, the EMOS platform, developed at the Eurecom Institute was presented. A description of the platform and all the procedures adopted for channel estimation and capacity calculation was detailed. To illustrate the EMOS, some channel estimation and capacity results were also presented.

As expected, the MIMO performance was shown to be

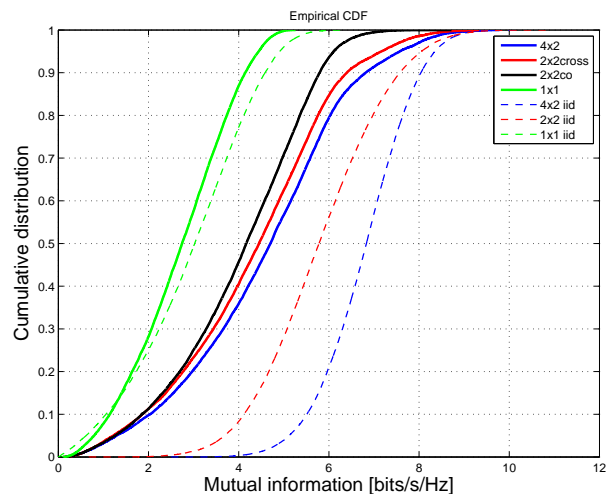


Fig. 9. Capacity for a given SNR (10dB).

indeed greater than the SISO one. However, the gain is less than the i.i.d. case. Moreover, cross-polarized antennas were shown to nearly double the capacity in comparison of the SISO case.

Many developments and studies are envisioned for the continuation of the EMOS project, including the evaluation of the impact of several scenario characteristics on the capacity and the effect of multiple users. Further developments include the enabling of multiple user channels, uplink-downlink operation as well as the evaluations of algorithms that efficiently exploit the gains provided by MIMO.

## ACKNOWLEDGMENT

The authors wish to thank Dr. Maxime Guillaud and Dr. Helmut Hofstetter for the initial development of the EMOS and for the insightful discussions.

## REFERENCES

- [1] I. Telatar, "Capacity of multi-antenna gaussian channels," *AT&T Technical Memorandum*, June 1995.
- [2] G. F. Foschini and M. J. Gans, "On limits of wireless communications in a fading environment when using multiple antennas," *Wireless Personal Communications*, pp. 6:311-335, August 1998.
- [3] H. Bolcskei and A. J. Paulraj, "Space-frequency coded broadband OFDM systems," *Wireless Communications and Networking Conference*, vol. 1, pp. 1-6, September 2000.
- [4] A. Molisch, M. Steinbauer, M. Toeltsch, E. Bonek, and R. Thom, "Capacity of MIMO systems based on measured wireless channels," *IEEE Journal on Selected Areas in Communications*, vol. 20, pp. 561-569, September 2002.
- [5] (2006) The OpenAir Interface website. [Online]. Available: <http://www.openairinterface.org/>
- [6] M. Wetterwald, C. Bonnet, H. Callewaert, L. Gauthier, R. Knopp, P. Mayani, A. Menouni Hayar, and D. Nussbaum, *UMTS-TDD software radio platform*. Chapter of "Reconfigurable Mobile Radio Systems :A Snapshot of Key Aspects Related to Reconfigurability in Wireless Systems" by Vivier, Guillaume (Ed), Apr 2007.
- [7] C. Bonnet, L. Gauthier, P. A. Humblet, R. Knopp, A. Menouni Hayar, Y. Moret, A. Nordio, D. Nussbaum, and M. Wetterwald, "An all-IP software radio architecture under RTLlinux," *Annales des télécommunications Volume 57, n7-8, juillet-août 2002*, 2002.
- [8] (2005) Eurecom Dual-RF CardBus/PCMCIA Radio Equipment. [Online]. Available: [http://www.openairinterface.org/docs/CardBus\\_MIMO\\_I.doc](http://www.openairinterface.org/docs/CardBus_MIMO_I.doc)